Impact of Fiber Dispersion on the Dynamic Range of a Static-Gain Burst-Mode Receiver for C-band 200G Upstream Coherent PON

Jad Sarkis
Optical Technology Laboratory
Huawei Heisenberg Research Center[1,]*
Munich, Germany
jad.sarkis@huawei.com
[*]also with: Politecnico di Torino[2]

Robert Palmer
Optical Technology Laboratory
Huawei Heisenberg Research Center[1]
Munich, Germany
robert.palmer@huawei.com

Giuseppe Talli
Optical Technology Laboratory
Huawei Heisenberg Research Center[1]
Munich, Germany
giuseppe.talli@huawei.com

Maxim Kuschnerov
Optical Technology Laboratory
Huawei Heisenberg Research Center[1]
Munich, Germany
maxim.kuschnerov@huawei.com

Valter Ferrero
Department of Electronics and Telecommunication
Politecnico di Torino[2]
Turin, Italy
valter.ferrero@polito.it

Roberto Gaudino
Department of Electronics and Telecommunication
Politecnico di Torino[2]
Turin, Italy
roberto.gaudino@polito.it

***Abstract*—We model a C-band 256 Gbps upstream (US) passive optical network (PON) link and a burst-mode coherent optical line terminal (OLT) receiver (RX) operating in static-gain mode. Specifically, we analyze the supported dynamic range (DR) penalty arising from fiber chromatic dispersion and its mitigation via chirped data transmission. By accepting analog-to-digital converter (ADC) clipping of the received high-power bursts, we demonstrate through simulation a burst-mode coherent RX supporting a 27 dB DR over a 100 km fiber link, without power leveling at the OLT RX or the optical network unit (ONU) transmitter. This work proves the feasibility of using commercially available coherent receivers for 200G-PON links.**

Keywords—Coherent PON, upstream, burst mode

I. Introduction

The rapid deployment of physical AI systems across residential and industrial environments is expected to drive unprecedented demands for US network capacity. This deployment comes with a reversal of traffic patterns from the human-centric, downstream-heavy traffic to the machine-driven, upstream-heavy one. Applications such as real-time 3D digital twinning, high-fidelity robotic perception, and AI factories now require the continuous upload of multi-sensor data, including 4K/8K vision streams and LIDAR point clouds, to edge-based or centralized reasoning engines. To meet these escalating performance demands, next-generation PON architectures must evolve to provide 200 Gbps US net capacity, as currently discussed in the ITU-T and FSAN Very High Speed PON (VHSP) initiative [1]. Intensity-modulation direct-detection systems, used for previous PON generations, face challenges reaching 200 Gbps per wavelength, mainly due to the high sensitivity requirements in PON point-to-multi-point topologies and their difficulties in handling chromatic dispersion (CD) and polarization mode dispersion at the required high symbol rate. In contrast, coherent technology offers both high sensitivity and digital dispersion compensation, allowing for a net 200 Gbps rate (after removal of overhead for framing and error correction), but the cost of the transceivers remains one of the challenges for its adoption in access networks. Moreover, the lack of coherent receivers with burst-mode transimpedance amplifiers (TIA) that can operate with a wide input DR is considered another limiting factor for the use of coherent transmission in access networks, where burst-mode operation is typically used in US. Possible options that have been recently studied to mitigate the high DR requirement at the receiver are often related to transmitter (TX) power pre-leveling at the ONU using SOAs [2], although this approach would add significant complexity to ONUs. Recently, a static gain coherent receiver has been experimentally demonstrated, enabling 20 dB of DR at 256 Gbps and 40 km of single-mode fiber (SMF) by tolerating clipping of high input powers [3]. This solution has the advantage of not requiring a centralized control of the ONU TX power and allows leveraging existing coherent receivers. This work extends this study by investigating, in simulation, the effects of CD on the DR of a commercial coherent receiver with static gain. We adopt the clipping-tolerant DP-QPSK modulation and tolerate up to 50% of TIA output clipping, accommodating burst power differences of up to 27 dB at the OLT receiver over a 100 km fiber link.

II. Simulation Setup and Receiver Model

In this section, the simulation setup and the model of the burst-mode coherent receiver are described. Some components of the receiver, namely, photodiode (PD), TIA and ADC, are of particular interest to this study as they have a direct impact on the supported DR. Their models will be detailed in subsection *B*.

A. Simulation setup

We use a custom Python-based simulation framework for studying the performance of the 200G burst-mode receiver. The schematic of the simulation setup is depicted in Fig. 1. The relevant parameters of the modeled components are listed in TABLE I. The simulation is performed in the time domain, using complex baseband signals. An offline digital signal processing (DSP) engine is used for sample generation and reception. Each burst comprises a constant amplitude zero auto-correlation (CAZAC) preamble [4], of 160 ns length, used for burst detection and channel estimation. Digital twins of the components in the analog channel, such as the digital-to-analog converter (DAC), driver, DP-IQ

978-3-903176-78-2 © 2026 IFIP

modulator, coherent receiver, and ADC have been implemented in Python based on analytical models. The multipoint-to-point fiber link has been modeled via CD emulation and a 120° state-of-polarization (SOP) rotation, while assuming optical launch powers below the nonlinear threshold of the fiber. A variable optical attenuator (VOA) after each ONU is used to control the respective burst powers into the coherent OLT RX. The output of the 4-channel ADC is connected to the offline RX DSP, where CD compensation, frame detection and alignment, frequency offset correction, timing and phase recovery and equalization are performed. The bit error rate (BER) is computed as a signal quality metric. In this simulation setup, the OLT RX receives interleaved bursts coming from two distinct ONUs with different adjustable received optical power, thus allowing us to evaluate the capability of the OLT in handling bursts at a varying DR.

B. Burst-mode coherent receiver model

The model of the OLT RX mimics a standard class-40 commercial integrated coherent receiver as described in [5]. Its key elements are the 90° hybrids, balanced PDs, TIAs, and ADCs. The PDs have an assigned input-referred responsivity, reflecting the combination of PD responsivity and insertion and excess loss of the 90° hybrids, (polarization) beam splitters (PBS, BS), and fiber-chip coupling. The TIA model comprises thermal noise addition, a nonlinear transfer function, and filtering. The thermal noise is modeled as additive white Gaussian noise (AWGN), with variance σ^2_{TIA}:

$$\sigma^2_{\mathrm{TIA}} = i^2_{\mathrm{irnd}} \cdot \Delta f, \qquad (1)$$

where Δf is the receiver's one-sided bandwidth and i^2_{irnd} is the one-sided differential input-referred noise current density. As in [6], we model the TIA transfer function by a tanh-function:

$$V_{out}(I_{in}) = V_{sat} \cdot tanh\left(\frac{Z_t \cdot I_{in}}{V_{sat}}\right), \qquad (2)$$

where V_{sat} is the saturation output voltage, Z_{t} is the transimpedance gain, and I_{in} is the input current. A Gaussian filter is used to limit the TIA's bandwidth. The ADC with differential input is modeled as a linear detector, clipping the input at $V_{\mathrm{ADC,max,pp}}$. Its quantization noise is modeled as AWGN with variance σ^2_{ADC}:

$$\sigma^2_{\mathrm{ADC}} = \frac{V^2_{\mathrm{ADC,max,pp}}}{2^{2 \cdot ENOB} \cdot 12}, \qquad (3)$$

with ENOB being the effective number of bits of the ADC and $V_{\mathrm{ADC,max,pp}}$ its peak-to-peak detection range.

TABLE I: SIMULATION PARAMETERS

Parameter	Value	Parameter	Value
Symbol rate	64 GBd	RRC roll-off	0.2
DAC sampling rate	120 GSps	ADC sampling rate	96 GSps
TX, RX laser power	16 dBm	Laser linewidth	100 kHz
TX, RX wavelength	1550 nm	Laser RIN	-155 dB/Hz
PD input referred responsivity	67 mA/W	TIA input referred noise	16 pA/√Hz
TIA transimpedance	5 kΩ	TIA V_{sat}	1.5 V
TIA bandwidth	40 GHz	ADC bandwidth	40 GHz
ADC $V_{\mathrm{ADC,max,pp}}$	1 V	ADC ENOB	5.5
DAC bandwidth	50 GHz	SOP	120°
Chromatic dispersion of fiber	17 ps/nm/km	Dispersion slope of fiber	0.06 ps/nm²/km

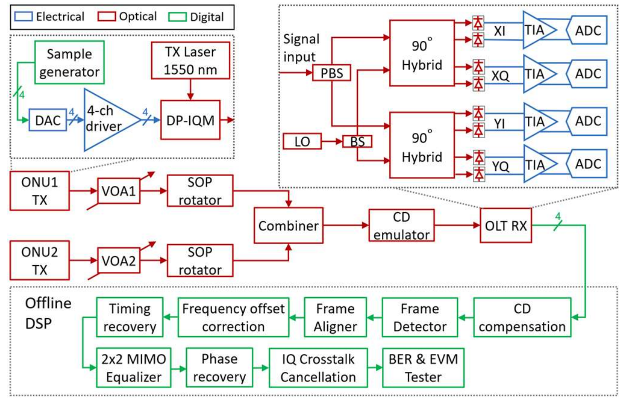

Fig. 1. Schematic of the simulated upstream 200G burst-mode US PON link, consisting of 2 ONU TXs and 1 OLT RX.

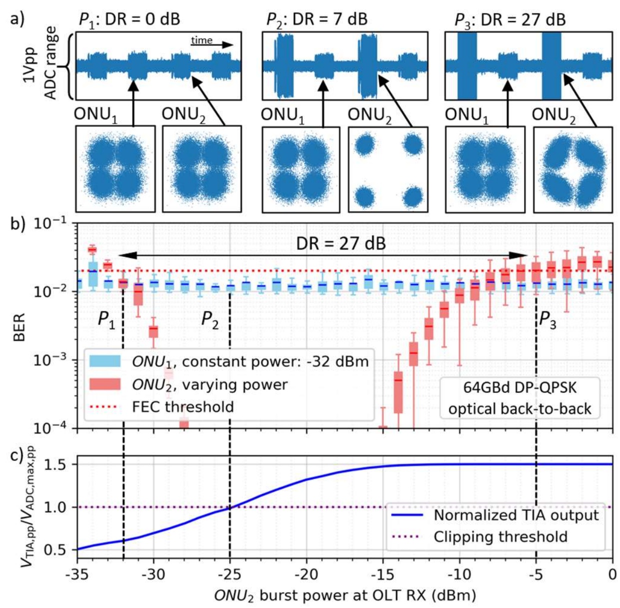

Fig. 2. (a) ADC capture of received bursts and recovered constellations at three dynamic range values, 0 dB, 7 dB and 27 dB. (b) Dynamic range sweep: ROP of ONU_1 bursts fixed to -32 dBm while the ROP of ONU_2 bursts varies. Blue and red boxplots show ONU_1 and ONU_2 burst performance, respectively. (c) Normalized TIA peak-to-peak output swing.

III. BACK-TO-BACK DYNAMIC RANGE MODELLING

The supported DR of the OLT RX in back-to-back (B2B) is evaluated when no CD is present. The VOAs maintain the OLT received power of ONU_1 bursts at -32 dBm, close to the RX sensitivity, while varying the power of the ONU_2 bursts from -35 dBm up to 0 dBm. The TX ON/OFF ratio of the ONUs is set to 54 dB, following the 50G-PON standard (see table 9-7 in [7]). For every VOA setting, the OLT captures 48 simulated bursts of 0.92 µs duration from each ONU. The burst power sweep is depicted in Fig. 2(b). Boxplots are used to illustrate the BER distributions for each burst power. The DR is defined as the power ratio between soft and loud bursts, and the OLT is considered to support a given DR if the mean BERs of soft and loud bursts are both below the forward error correction (FEC) threshold of 2×10^{-2} (a threshold assumed in most VHSP investigations and compatible with O-FEC [8] and SD-LDPC [9]). There are three distinct regimes that can be observed in Fig. 2(b). The first one is at low ROP for both ONUs, where reception is limited by the TIA thermal noise and ADC quantization noise (see setting P_1). The RX sensitivity can be estimated as -32.7 dBm at the set TIA gain. At setting P_2, the signal-to-noise ratios of the ONU_2 bursts increase and clipping has not yet occurred. Increasing the burst power of ONU_2 further, leads to ADC clipping and TIA-induced nonlinearities. Thus, at setting P_3, the TIA output peaks of the loud bursts are clipped by 50% by the ADC, significantly degrading the performance. Despite the heavy clipping at high ROP, the simulation shows a reception range from -32.7 dBm to -5.7 dBm supporting operation at a DR of 27 dB, which is 7 dB above the typical 20 dB DR requirement from high-speed PON standards [7].

IV. Effect of Chromatic Dispersion on DR

Coherent DSP is known for efficient receiver-side CD compensation with low transmission penalties when working with a linear transmission channel. In this work, however, loud bursts may be clipped or suffer from the TIA nonlinearities, which is expected to lead to a penalty when applying RX CD compensation. We emulate SMF28 fiber lengths of up to 100 km in C-Band by sweeping the emulated CD value from 0 ps/nm to 1700 ps/nm in steps of 17 ps/nm. In each step, a DR sweep as depicted in Fig. 2(b) is performed.

A. *RX CD compensation*

The measured DR of the RX as a function of CD is depicted in Fig. 3(a). As expected, the lower detection threshold is independent of the CD in the link, due to the operation in the linear regime. In contrast, the upper detection threshold is highly sensitive to CD, with a peak-to-peak variation of 10 dB, due to the nonlinear operation regime of the RX. There is no monotonic relationship between CD and upper threshold. Instead, several valleys of the upper threshold can be found, particularly centered around 12 km and 80 km. The secondary y-axis illustrates the peak-to-average power ratio (PAPR) of the TIA output (at -16 dBm input power) as a function of CD. It can be seen that the PAPR initially increases as CD is added. Overall, we find a good anticorrelation between PAPR and the upper detection threshold. The increase in PAPR (for constant average burst power) leads to an increase in clipping at the ADC and therefore to more nonlinearities, reducing the upper detection threshold.

B. *TX CD pre-compensation*

The CD-related penalties can be mitigated by pre-compensating the CD in the TX DSP by chirping the TX waveform with an all-pass filter of phase response opposite to that of the fiber. This digital filter, however, increases the PAPR of the TX output. The TX signal is clipped to a maximum PAPR of 9 dB by the DAC. Consequently, the TX output power drops by up to 3 dB, then remains constant for CD pre-compensation values above 70 ps/nm, as depicted in Fig. 3(c). This power loss could be mitigated using a semi-conductor optical amplifier at the ONU. The matched CD pre-compensation leads to an approximately constant PAPR at the OLT receiver, as depicted in Fig. 3(b), and the fluctuations of the resulting upper reception threshold are effectively reduced from 10 dB to 2.6 dB. The DR becomes approximately 27 dB over the entire simulated CD range.

Conclusion

We have demonstrated a C-Band 256 Gbps burst-mode coherent PON US link with up to 100 km SMF reach,

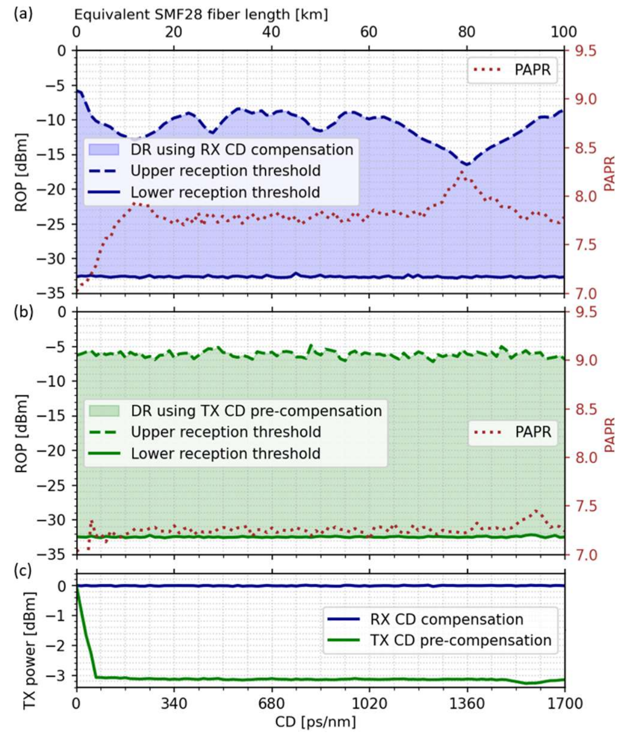

Fig. 3. Simulated DR of the static-gain burst-mode RX as a function of RX compensated CD (a) The lower reception threshold (linear regime) is constant, while the upper reception threshold (clipping regime) is fluctuating as a function of the TIA output PAPR. (b) Digital CD pre-compensation at the TX, leading to constant PAPR at the TIA output and flat upper reception threshold. (c) TX output power as a function of pre-compensated CD.

capable of supporting a dynamic range of up to 27 dB at the OLT RX, without any power leveling at the OLT receiver or ONU transmitter. Penalties related to CD compensation in the clipping regime of the receiver have been effectively overcome by means of transmitting a digitally chirped signal. The use of chirping makes the supported DR independent of the link's CD, at the cost of increasing the modulation loss by 3 dB due to an increased TX PAPR. This finding supports the possibility of using commercial coherent receivers for 200G-PON US links.

References

[1] D. Zhang et al., "Progress of Very High Speed PON in ITU-T [Invited]," *J. Opt. Commun. Netw.*, vol. 18, no. 2, p. A112, Feb. 2026.

[2] K. Vijayan et al., in *OFC 2025*, doi.org/10.1364/OFC.2025.M2I.2

[3] J. Sarkis *et al.*, "Experimental Demonstration of a Large Dynamic Range Burst-Mode Receiver for 200G Upstream Coherent PON Based on Static Gain TIA," in *OFC 2026*, p. W4F.1

[4] D. Chu, "Polyphase codes with good periodic correlation properties (Corresp.)," *IEEE Trans. Inf. Theory*, vol. 18, no. 4, pp. 531–532, Jul. 1972, doi: 10.1109/TIT.1972.1054840.

[5] *Implementation Agreement for Micro Intradyne Coherent Receivers*, 2017. [Online]. Available: https://www.oiforum.com/wp-content/uploads/2019/01/OIF-DPC-MRX-02.0.pdf

[6] K. Abdelfattah and B. Razavi, in *IEEE Custom Integrated Circuits Conference 2006*, San Jose, CA: IEEE, Sep. 2006, pp. 197–200. doi: 10.1109/CICC.2006.320908.

[7] *ITU-T G.9804.3: 50-Gigabit-capable passive optical networks (50G-PON): Physical media dependent (PMD) layer specification*. [Online]. Available: https://www.itu.int/rec/T-REC-G.9804.3/en

[8] *Open ZR+ MSA Technical Specification*. [Online]. Available: https://openzrplus.org/wp-content/uploads/2024/04/openzrplus_rev3p0_final2.pdf

[9] M. Yang et al., "Real-Time Verification of Soft-Decision LDPC Coding for Burst Mode Upstream Reception in 50G-PON," *J. Light. Technol.*, vol. 38, no. 7, pp. 1693–1701, Apr. 2020.